NUMERICAL PREDICTION EXPERIMENT OF AN ADVECTION FOG IN NANLING MOUNTAIN AREA*

FAN Qi (樊 琦), *WANG Anyu* (王安宇), *FAN Shaojia* (范绍佳),

Department of Atmospheric Sciences, Zhongshan University, Guangzhou 510275

WU Dui (吴 兑), *DENG Xuejiao* (邓雪娇)

Guangzhou Institute of Tropical and Oceanic Meteorology, Guangzhou 510080

and *LIU Yingwei* (刘英伟)

Macau Meteorological and Geophysical Services, Macau

Received November 28, 2002; revised March 10, 2003

ABSTRACT

Now more comprehensive cloud microphysical processes have been included in advanced three-dimensional mesoscale meteorological model such as PSU/NCAR MM5 model, so the model can be used in the prediction of fog. In this paper, MM5 was utilized to simulate an advection fog occurring in Nanling Mountain area. The simulated results were compared with the facts obtained by detailed observation experiment. The results showed that the simulation was successful in the following aspects: (1) the formation and development of the fog; (2) the temporal variation of the maximum liquid water content; (3) the diffusion of the cold air, especially the temporal variation of the ground temperature; and (4) the uplift of the air and the formation and development of the low-lever inversion. Besides, we did some sensitivity numerical experiments and discussed the effects of the radiation, the release of condensation latent heat and the change of soil moisture and temperature on the formation and development of fog. The success of numerical simulation experiment of fog has proved that the numerical forecasting of fog is promising.

Key words: Nanling Mountain, advection fog, numerical simulation, sensitivity experiments

I. INTRODUCTION

With the development of the highway, more attention has been paid to the prediction of fogs. Since the fog model has first been set up by Fisher and Caplan (1963), the research on the numerical simulation of fogs has been developed rapidly. One or two-dimensional fog model was used in the study on the fog by Fisher and Caplan (1963), Zdunkowski and Nielsen (1969), Roach and Brown (1976). Recently Zhou (1987), Qian et al. (1990), and Zhang et al. (1993) also analyzed the formation and dissipation of the fog using one or two-dimensional fog model. After 1990, Shi et al. (1996) and Huang et al. (2000) have done numerical simulation researches on the radiation fog using a three-dimensional fog model. They all achieved many meaningful results. One of the objectives of the numerical simulation researches is to do the numerical prediction. In recent years,

* This study was supported by the National Key Project ZKCX2-SW-210 of Chinese Academy of Sciences and the National Natural Science Foundation of China (49975001).

the numerical prediction models have got rapid progresses (White et al. 1999). For example, a comprehensive cloud microphysical process has been included in the fifth-generation NCAR/Penn State mesoscale numerical prediction model (MM5) (Grell et al. 1995), cloud water and rain water are taken as predictors, the falling speed of the rain drop and the auto-conversion between cloud drop and rain drop are computed in the moisture prediction equations. Obviously, it will contribute to the numerical simulation of fogs. Macau Meteorological and Geophysical Services have introduced MM5 model and took the model as their own operational numerical prediction model (ESCAP/WMO Typhoon Committee 2000). We did several numerical simulation experiments of the fog using this model and all had success. Before 1990 only fog models were used to research the fog cases. In 1991, Balland et al. (1991) conducted the first attempt to use the United Kingdom Meteorological Office mesoscale model to simulate the fog over northeast Scotland. Using MM5 mesoscale model we have performed some successful fog simulation experiments. The results of the experiments will be shown as follows.

There have many fog events in winter and spring in Nanling Mountain area. Most are advection fogs and have a long duration and a low visibility. Beijing-Zhuhai highway from south to north passes through Nanling Mountain. The prediction of the heavy fog is very important to the security of the traffic. In the following, we will discuss a short-term numerical simulation experiment of an advection fog occurring in Nanling Mountain area using MM5 model. We can compare the numerical simulation results with the observations carefully. Because we did detailed observation experiment on this fog case, thus many valuable data were obtained (Tang et al. 2002).

The simulation experiment is successful, and then we did some sensitivity numerical experiments, then discussed the effects of radiation, and the release of latent heat, and the change of the soil moisture and temperature on the fog formation and development.

II. MODEL, DATA AND SCHEMES OF NUMERICAL EXPERIMENTS

MM5 model developed very fast in recent years. The MM5V3. 4 version we used not only included the comprehensive cloud microphysical process but also included the OSU/Eta land-surface model (Chen and Jimy 2001a; 2001b) and the new longwave radiation scheme developed by AER Inc (Mlawer et al. 1997). The above stated land-surface model has included a canopy layer and four prognostic variables: soil moisture and temperature in the soil layer, water stored on the canopy and snow stored on the ground. The soil is divided into four layers and the depth of each layer downward from the ground surface is 10 cm, 30 cm, 60 cm and 1 m, the soil types are divided into 14 kinds. This scheme has obvious influences on the computation of the surface sensible heat and latent heat. It greatly improved the computation and prediction of the heat balance on the underlying surface. The new longwave radiation scheme has included the rapid radiation transfer model and used a correlated-k model to represent the effects of the detailed absorption spectrum taking into account water vapor, carbon dioxide and ozone. It is a highly accurate and efficient method. From the following numerical experiment results, we can see that it is important to the simulation of fog to introduce the OSU/Eta land-surface model and the new longwave radiation scheme.

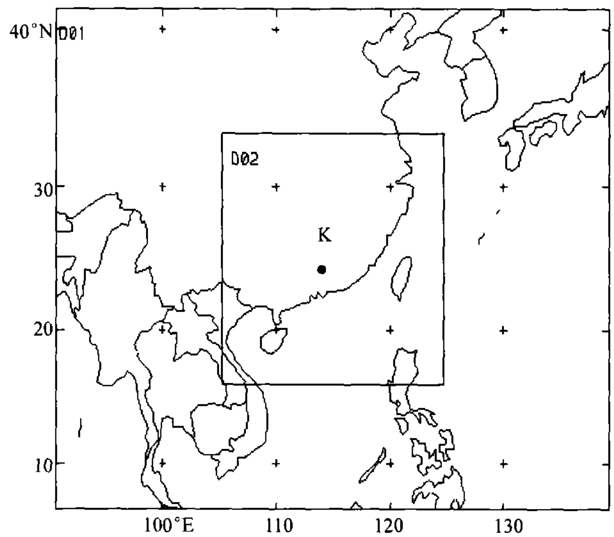

Fig. 1. The selected domains in our experiments (black dot K denotes the Kaifeng Primary School).

For the physical options, besides the OSU/Eta land-surface model and the new longwave radiation scheme, Grell cumulus convection parameterization scheme, warm rain explicit moisture scheme and MRF planetary boundary layer scheme are chosen in our simulation experiments. The selected domains in our experiments are shown in Fig. 1. We chose the location of the center site in the domain nearby the Kaifeng Primary School in Yunyan Town in Lechang City (25°N, 115°E), which is our observational site. Two nesting techniques are used in the experiment. Horizontal grid distances are 54 km and 18 km respectively (Fig. 1). The vertical resolution is 23 layers and the top level 100 hPa.

The observational site is at 25.1°N, 113.1°E (Fig. 1) and its height above sea level

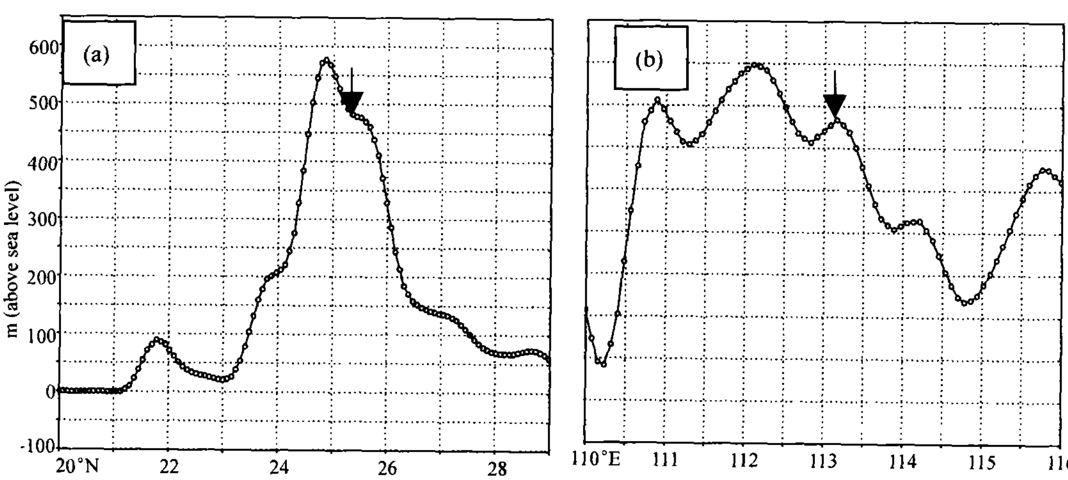

Fig. 2. The topography of the observational site: (a) the meridional topography distribution along 113.1°E; (b) the zonal topography distribution along 25.1°N, the arrow denotes the site in the Kaifeng Primary School.

(asl) is 815 m. The horizontal distance from the observational site to the highest tip of that highway over Nanling Mountain is 100 m or so, and the observational site is very close to that highway. Figure 2 is the topography of the observational site in MM5 model. It is similar to the actual topography but the height of about 550 m is some lower. There are many advanced instruments besides the routine meteorological observation in our observational site for fog observation, such as digital microphotography, hot-wire liquid water content meter, wiresonde, dual sounding and so on.

For numerical experiments of fog the initial and boundary data are taken from the NCEP/NCAR daily $2.5^{\circ}\times 2.5^{\circ}$ grid-data, including the initial value of soil moisture and soil temperature. Numerical simulation starts at the 2000 local time (1200 UTC) 6 March, 2001 and ends at 2000 LT 7 March.

III. THE OBSERVATIONS OF THE DENSE FOG PROCESS IN NANLING MOUNTAIN AREA ON MARCH 7, 2001

On March 7, 2001, a dense fog appeared in the Nanling Mountain area. The southward cold air encountered the northward moist warm air in the area and caused the fog. This fog belongs to an advection fog. It was shown from the observations that the wind direction is by south in the Kaifeng Primary School before 0000 LT 7 March. About 2300 LT 6 March the wind direction was SSW and the wind speed was 2 m/s. At that time stratocumuli clouds appeared in the lower troposphere. The air near the surface was very damp and warm. The air temperature was 13.8℃ and the air humidity was 97%. About 0200 LT 7 March, the dense fog formed and the wind fell down. The air temperature started to fall and the humidity rose up to 100%. The visibility fell to 200 m. About 0500 LT, wind direction started to change from by south to by north (NNW). At that time it started to rain. From 0700 to 0800 LT the rainfall was 1.4 mm/h that was the maximum of the drizzle caused by fog on March 7. The air temperature fell fast and it was about 8℃. Because of the drizzle, the dense fog thinned between 0500 and 0700 LT. After 0700 LT, the wind started to fall. The falling of the temperature became to slow and the fog became thicker. About 0830 LT, the visibility fell to below 200 m. Meantime it started to rain and because of the drizzle the fog became thinner again. It should be pointed out that this situation happened repeatedly, that is, because of the drizzle the dense fog thinned, and vice versa. The secondary peak of the drizzle occurred at 1400 LT. It reached 0.5 mm/h and the visibility was near 800 m. The total decrease of temperature was no more than 1℃ from 0700 to 2100 LT. The evolutions of the fog droplet spectrum were very consistent with the visibility (not shown). The spectrum of fog droplets widens and the number of fog droplets decreases when the visibility increases, and vice versa.

Figure 3 is the time-height section of the observed temperature and dewpoint for the fog case. From Fig. 3a, we can see that the low-level inversion did not appear at 2300 LT 6 March and all the air was saturated in the lower troposphere. But it is a pity that there are no observational data at 0200 LT 7 March. In Fig. 3, the low-level inversion appeared obviously at 0700, 1100 and 1700 LT. In Fig. 3c and Fig. 3d, the air was not saturated at heights higher than 2 km.

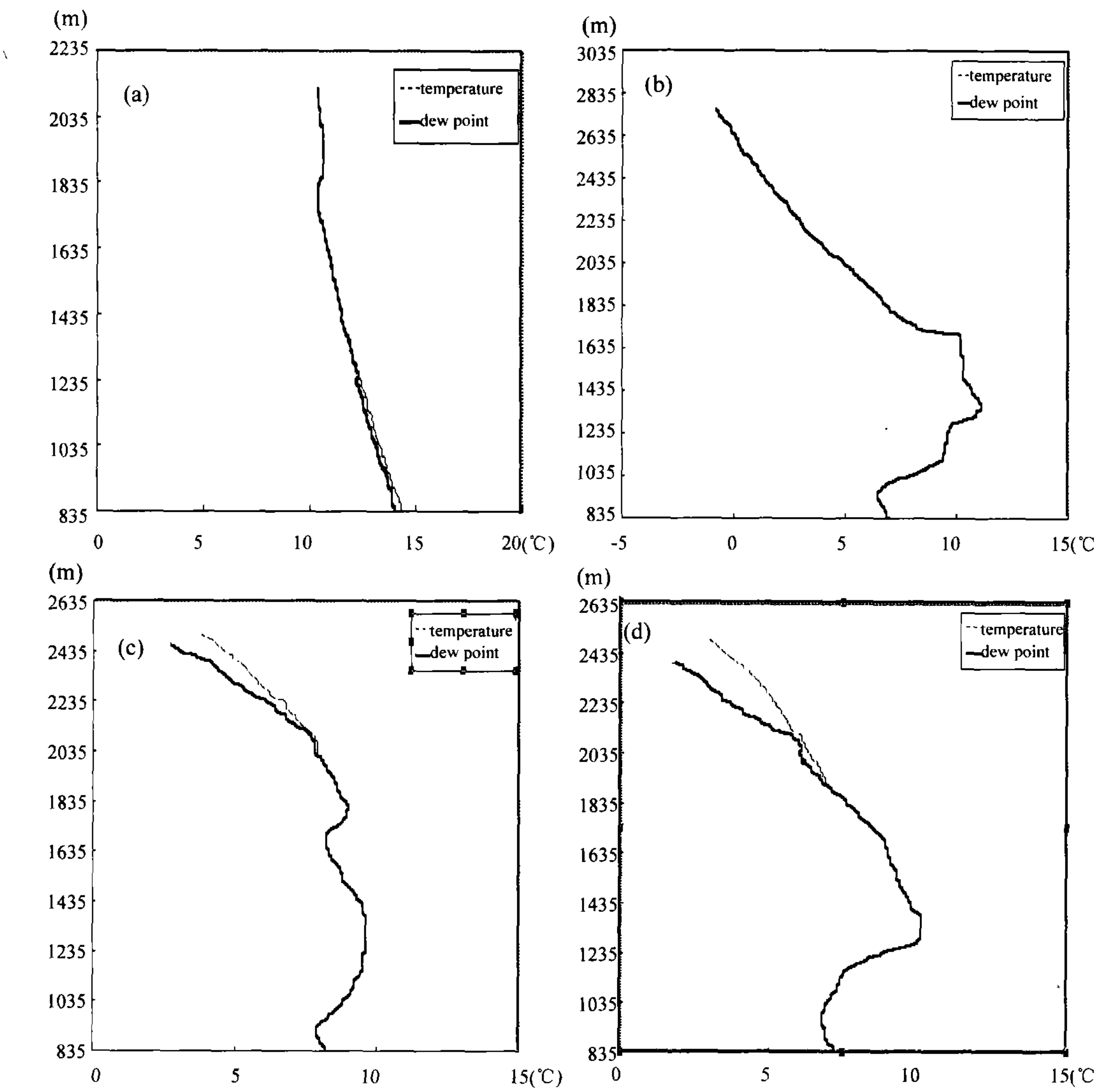

Fig. 3. The time-height sections of the observed temperature and dew point at (a) 2300 LT 6 March, (b) 0700 LT 7 March, (c) 1100 LT 7 March, and (d) 1700 LT 7 March.

IV. THE RESULTS OF THE PREDICTION EXPERIMENT

When the southward cold airflow encountered with the northward airflow, the condensation may happen and the fogs formed. Fogs and visibility were opposite. The denser the fogs are, the less the visibility is, and vice versa. Figure 4 is the time evolutions of the observed and simulated liquid water content and the observed visibility. The simulated liquid water contents described the maximum liquid water contents under 2 km height. As a rule, fogs are associated with the visibility below 1000 m. Light fog can be associated with the visibility between 1000 m and 2000 m (Tourskoi 1967). By the observational visibility, the fog formed at 0200 LT 7 March at the Kaifeng Primary School (our observational site) and maintained for one day. When the liquid water content is over

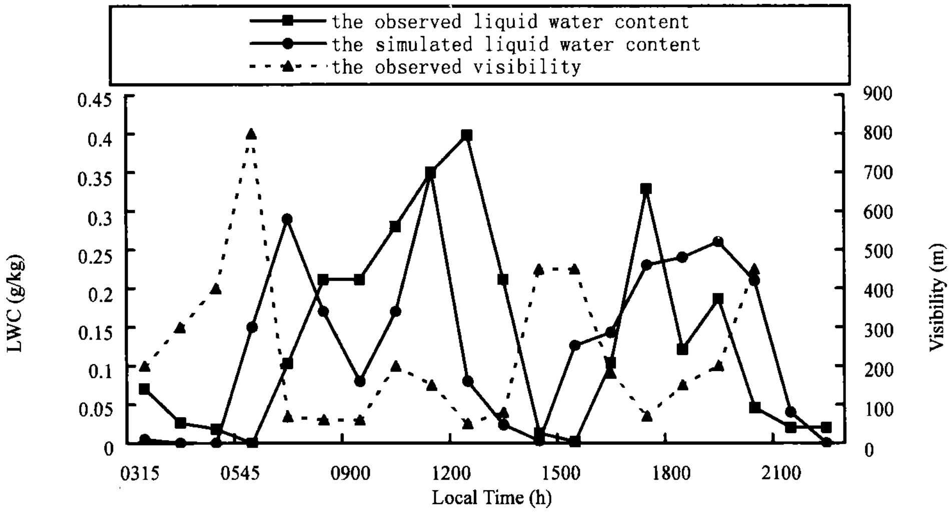

Fig. 4. Time evolutions of the observed and simulated liquid water content (LWC) and the observed visibility.

0.05 g/kg the fog will form (Cotton and Anthes 1993). From the observations, the fog formed at 0200 LT 7 March at the Kaifeng Primary School and disappeared three times at 0430, 1430 and 2100 LT, respectively (Fig. 4). The fog maintained for 15 hours, and the observational maximum of the liquid water content (LWC) was about 0.4 g/kg.

From Fig. 4 we can see that the numerical simulation experiment was successful. The simulated fog formed before 0500 LT and disappeared twice at 1330 and 2100 LT. It maintained for 14.5 hours. The maximum LWC reached 0.35 g/kg. The temporal variations of the simulated LWC were almost consistent with the observations. Both the observational and the simulated peak values of LWC were very similar.

Figure 5 is the time-height section of the simulated LWC nearby the Kaifeng Primary School. We can see from this figure that the temporal variation of the vertical distribution of the LWC of the fog. The average LWC of the stratocumulus cloud is about 0.3—0.5 g/kg (Fletcher 1966). The LWC in stratocumuli cloud is obviously higher than that in fog. In Fig. 5 there has a sheet of stratocumulus cloud above the fog. The height of the stratocumulus cloud is about 2000 m to 4000 m. Observational records showed that there had stratocumuli cloud in the sky of the Kaifeng Primary School. From Fig. 3a and Fig. 3b we can see that the air was saturated above 2000 m from 2300 LT 6 March to 0700 LT 7 March which was corresponding to the stratocumuli clouds. In Fig. 5 there has an obvious transition layer between stratocumuli cloud and fog.

The dew-point deficit was very small in fog region or cloud filed. Figure 6 is the time-height section of the simulated dew-point deficit. By comparing Fig. 6 with Fig. 3 it can be seen that the simulated results were in accord with the observations.

This fog case was associated with a diffused cold air. Before the formation of fog, the northward warm air at the Kaifeng Primary School was very active and the wind speed was about 3 m/s. When the southward cold air encountered with the warm air at midnight, the fog started to form. Figure 7 is the temporal variation of the simulated ground temperature and the observed air temperature at the Kaifeng Primary School. Recently a great

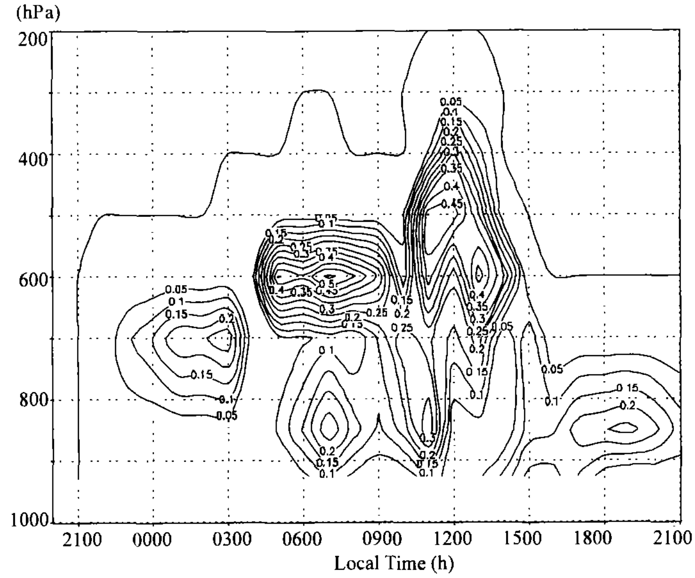

Fig. 5. The time-height section of the simulated LWC (g/kg) nearby the Kaifeng Primary School.

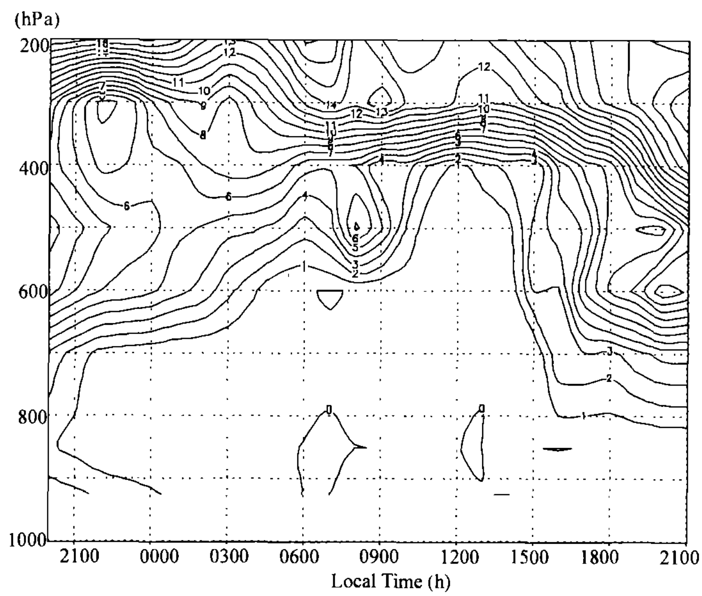

Fig. 6. The time-height section of the simulated dew-point deficit (°C).

improvement in ECMWF model is to add its vertical resolution and descend the lowest prediction layer to 10 m (Jakob et al. 2000), but in MM5 model it could not do it. Limited to the vertical resolution of the MM5 it could not give the simulated air temperature near the surface. But from Fig. 7 we can see that the simulated ground temperature was compared with the observational air temperature near the surface.

The ground and air temperatures near the surface are mainly influenced by three factors. The first is the diffusion of the cold air. The second is the longwave radiation. Both of the two factors can cause the fall of the ground and air temperatures near the surface. Before sunrise, with the influences of the diffusion of the cold air and longwave radiation the ground and air temperatures near the surface fell fast. The third factor is the

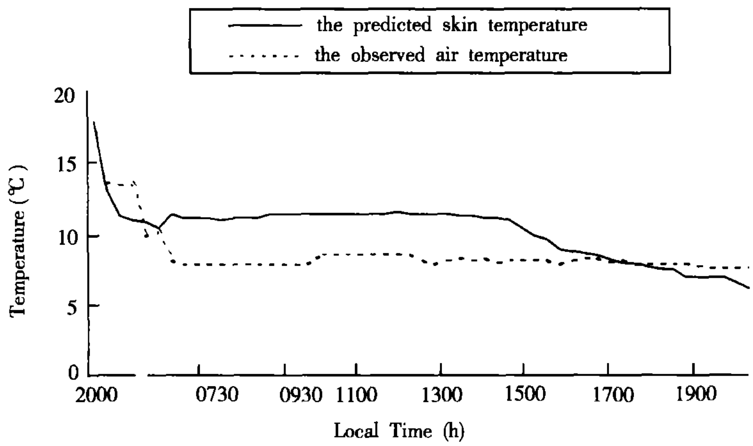

Fig. 7. The temporal variations of the simulated ground temperature and the observed air temperature at the Kaifeng Primary School.

shortwave radiation. The influence of the third factor is opposite to those of the former two factors so that after sunrise the ground and air temperatures near the surface have no much change. It goes without saying that the simulation of fog greatly depends on the prediction of ground and air temperatures near the surface.

Figure 8 is the vertical cross section of the simulated temperature and wind field in the north-south direction. At 2300 LT 6 March, before the formation of fog the cold air was very close to the Kaifeng Primary School and due to diffusion action its frontier was very thinner as shown in Fig. 8a. Fog started to form when the diffused cold air encountered with the warm air. Meantime the warm air started to uplift above the thinner cold air, which resulted in a low-level inversion layer near the surface. In Fig. 3b, the depth of this low-level inversion layer was about 400 m and the top of this inversion layer was near 850 hPa. The corresponding simulated depth (Fig. 8b) was much the same as that in Fig. 3b. Due to the lower terrain height in MM5 the simulated depth of the layer is also rather lower. During 0700 to 1100 LT 7 March, the cold air diffused southward continually and the warm air continued to uplift (Fig. 8c). Obviously it was favorable to the transformation of the cold air and the development of fog. After noon, the cold air diffused fast and stretched upward as shown in Fig. 8d and the fog started to dissipate.

The temporal resolution of the NCEP/NCAR data is 6 h. Figure 9 is the vertical cross section of the temperature and wind field calculated with the NCEP/NCAR data at 0800 and 2000 LT 7 March. The simulated results were similar to the results calculated with the corresponding NCEP/NCAR data. For example, in Fig. 9a and Fig. 8b it can be seen that obvious air rising motion is predominated in fog region at 0800 LT and in Fig. 9b and Fig. 8d there have been all controlled by north winds under 900 hPa. There has no obvious air rising motion in fog region. Because the horizontal and vertical resolutions of NCEP/NCAR data are lower than that in MM5 model, the horizontal resolution of the NCEP/NCAR data is 250 km and the vertical resolution under 100 hPa is 12 layers. But the horizontal resolution used in the experiment is 18 km and the vertical resolution is 23 layers in MM5. The lower resolution of NCEP/NCAR data has smoothed many local

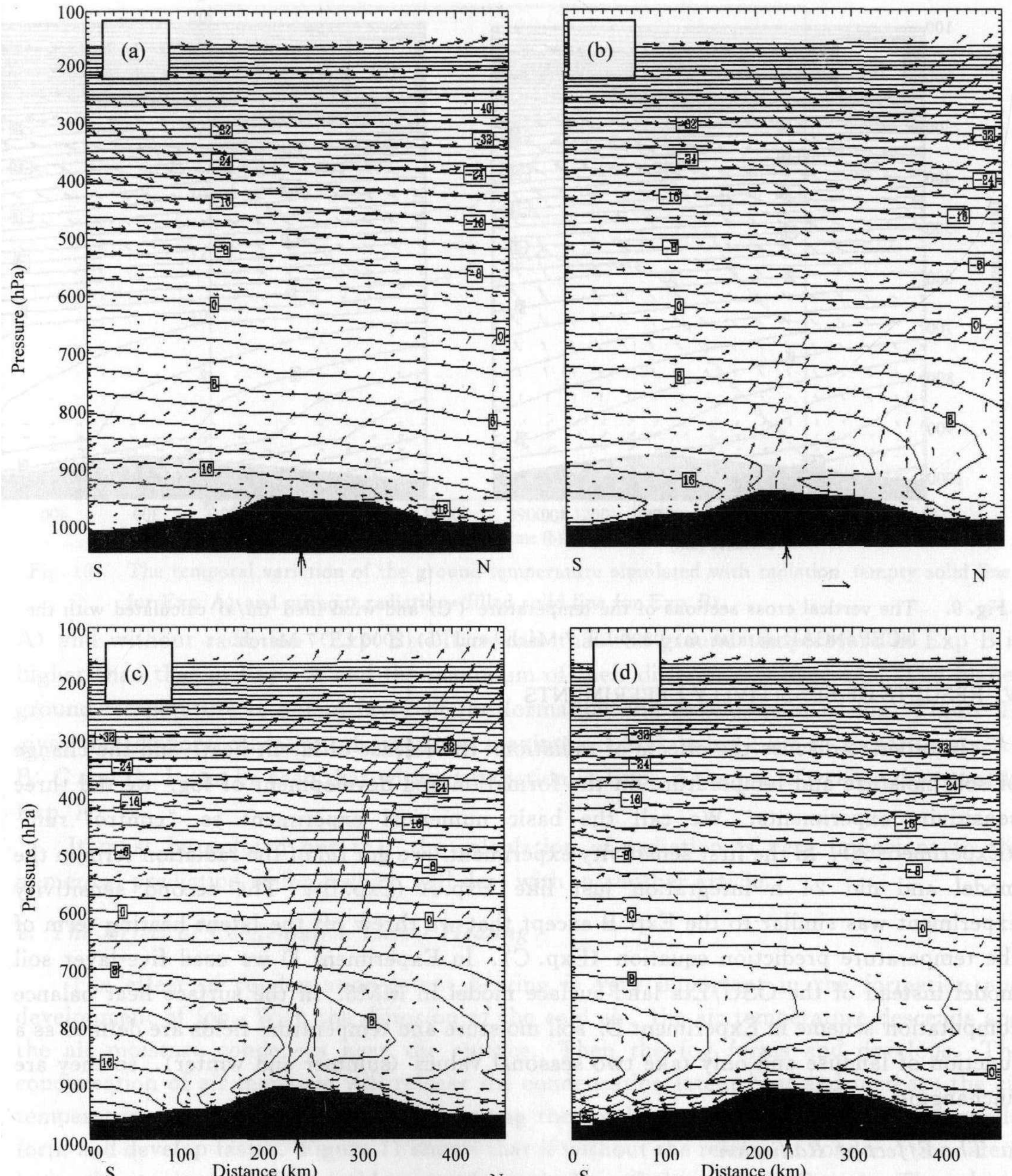

Fig. 8. The vertical cross sections of the simulated temperature (℃) and wind field (m/s) in the north-south direction. (a) 2300 LT 6 March; (b) 0700 LT 7 March; (c) 1100 LT 7, March, and (d) 1700 LT 7, March.

phenomena. We believe that the results simulated by the model may be close to the reality. For example, the low-level inversion layer observed by the radio soundings as shown in Fig. 3 can be simulated clearly in Fig. 8, but can not be seen in Fig. 9.

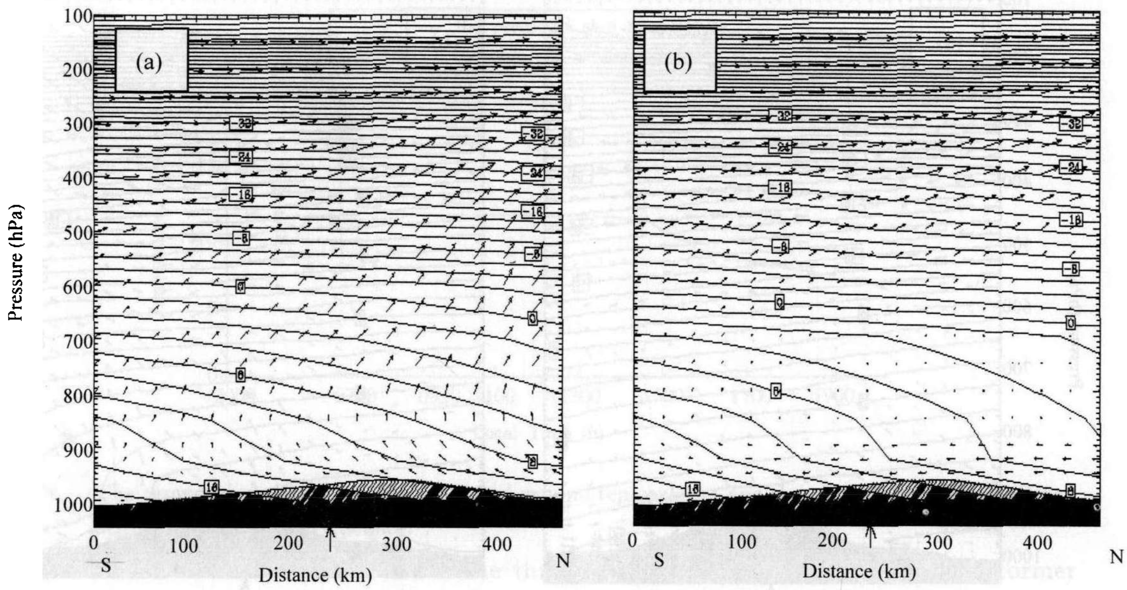

Fig. 9. The vertical cross sections of the temperature (℃) and wind filed (m/s) calculated with the NCEP/NCAR data at (a) 0800 LT 7 Mach, and (b) 2000 LT 7 March.

V. RESULTS OF SENSITIVITY EXPERIMENTS

In order to discuss the effects of radiation, the release of latent heat, and the change of soil moisture and temperature on the formation and development of fog, we did three sensitivity experiments. We call the basic numerical experiment as "control run" (Experiment A). In the first sensitivity experiment, we got rid of the radiation term in the model and did 24 h integration just like Exp. A (Exp. B). The second sensitivity experiment was similar to the Exp. B except that we threw off the latent heating term of the temperature prediction equation (Exp. C). In Experiment D we used five-layer soil model instead of the OSU/Eta land-surface model in MM5. In the surface heat balance computation scheme in Experiment D, soil moisture and temperature fields are defined as a function of landuse and only take two seasonal values (summer and winter), so they are unchanging.

1. *The Effect of Radiation*

During nighttime there is no solar radiation. For longwave radiation budget the downward value is smaller than the upward value at the surface, so that the ground and air temperatures near the surface descend by the effect of the longwave radiation. The descending of ground and air temperatures near the surface will cause the condensation of air moisture and the formation of fog. For mountain advection fog, the effect of radiation is also important. The descending of ground and air temperatures near the surface will benefit to the diffusion of the cold air. If without the effect of radiation, the ground temperature would be higher and then the diffusion of the cold air would be slower. Figure 10 shows the simulated temporal variation of the ground temperature with radiation (Exp.

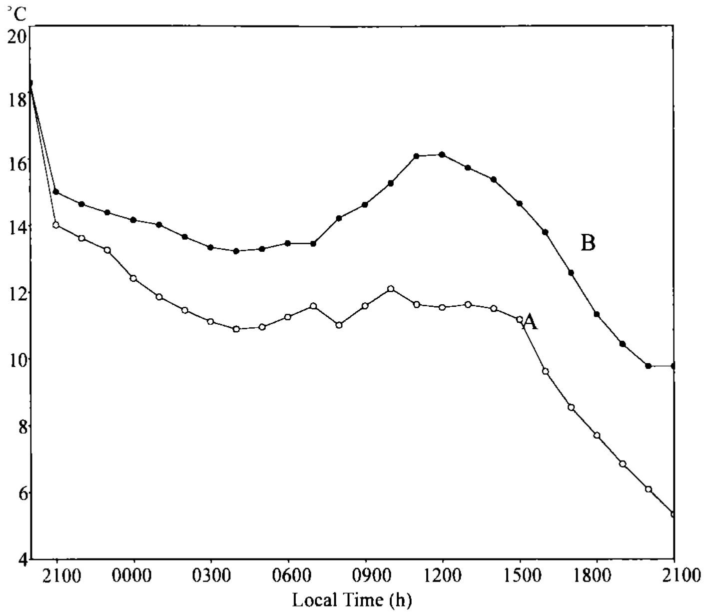

Fig. 10. The temporal variation of the ground temperature simulated with radiation (empty solid line for Exp. A) and without radiation (filled solid line for Exp. B).

A) and without radiation (Exp. B). It reveals that the ground temperature in Exp B is higher than that in Exp. A and the maximum of their difference is over 4℃. The higher ground temperature is not in favor of the formation and development of fog. Figure 11 gives the temporal variation of simulated maximum LWC under 2 km in Experiments A, B, C and D. It can be seen that without radiation in Exp. B the fog is weaker than that in Exp. A.

It must be pointed out that the calculation of radiation is very important to the numerical prediction of fog, which will deal with in another article.

2. *The Effect of Condensation Latent Heating*

The effect of condensation latent heating is very important in the formation and development of fog. With the diffusion of the cold air, the air temperature descends and the air moisture condenses near the surface. Then the fog forms and develops. The condensation of air moisture will release the condensation latent heat and increase the air temperature near the surface. So if removing the condensation latent heating, fog would form and develop faster. Figure 11 shows that if without the release of condensation latent heat, the maximum LWC would appear faster in Exp. C than that in Exp. A. The release of condensation latent heat has great effect on the formation and development of fog. In addition, the release of the condensation latent heat can cause the development of the updraft flow in fog region. We can see from Fig. 11 that after the formation of fog if there is no the effect of latent heat, the fog would form faster and dissipate faster too. The fog dissipated before noon in Exp. C. The duration of fog in Exp. A is longer than that in Exp. C.

3. *The Effect of the Change of Soil Moisture and Temperature*

For Exp. A the soil moisture and temperature are predictors in OSU/Eta land-surface

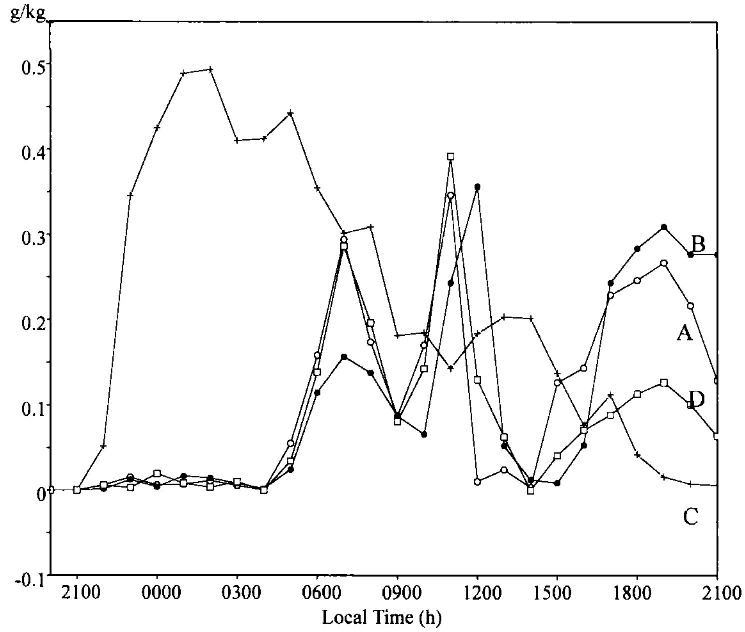

Fig. 11. The temporal variation of simulated maximum LWC under 2 km in Exps. A, B, C and D (the empty dot line for Exp. A, the filled dot line for Exp. B, the cross line for Exp. C, and the square line for Exp. D).

model. For Exp. D as stated above the soil moisture and temperature fields are unchanged. The change of soil moisture and temperature has contribution to the formation and development of fog.

According to the numerical experiment by Chen and Dudhia (2001a; 2001b), the soil moisture and temperature have obvious diurnal variation. There has maximum difference at 1800 LT between Exps. A and D. For Exp. A at about 1800 LT it would be in favor of the development of fog. Figure 11 shows that if the OSU/Eta land-surface model were not used, the fog after 1500 LT 7 March would not be simulated out.

VI. CONCLUDING REMARKS

A three-dimensional mesoscale meteorological model MM5 was used to simulate a 24-hour advection fog case occurring in Nanling Mountain area. The simulated results were compared with the facts obtained by detailed observation experiments. The success of numerical simulation experiment of fog has great significance for the numerical forecasting of fog. The results showed that the simulation was successful in the following aspects: (1) the formation and development of the fog; (2) the temporal variation of the maximum LWC of the fog; (3) the diffusion of the cold air, especially the temporal variation of the ground temperature; and (4) the uplift of the air and the formation and development of the low-level inversion. Besides, we also did some sensitivity numerical experiments and discussed the effects of the radiation, the release of condensation latent heat and the change of soil moisture and temperature on the formation and development of fog. The results showed that: (1) Even if this fog belongs to advection fog, the effect of the radiation is also important. If without radiation in MM5 model, the ground temperature would increase and the fog would become weaker. (2) The release of condensation latent heat has great effect on the formation and development of fog. If without the release of latent heat, the development of fog would be faster and the LWC would be higher than that in Exp. A. Compared with Exp. A the formation and development of fog is faster in Exp. C, and its duration of fog is shorter. (3) The difference between Exps. A and D mainly occurred at 1800 LT. For Exp. A at about 1800 LT it would be in favor of the development of fog. We hope to predict the fog case by mesoscale model in near future, and it is obviously promising.

REFERENCES

Ballard, S. P., Golding, B. W. and Smith, R. N. B. (1991), Mesoscale model experimental forecasts of the haar of northeast Scotland, *Mon. Wea. Rev.*, **119**: 2107—2123.

Chen, F. and Dudhia Jimy (2001a), Coupling an advanced land surface-hydrology model with the Penn State-NCAR MM5 modeling system, Part I: Model implement and sensitivity, *Mon. Wea. Rev.*, **29**: 569—585.

Chen, F. and Dudhia Jimy (2001b), Coupling an advanced land surface-hydrology model with the Penn State-NCAR MM5 modeling system, Part II: Preliminary model validation, *Mon. Wea. Rev.*, **29**: 587—604.

Cotton, W. R. and Anthes, R. A. (1989), *Storm and Cloud Dynamics*, Academic Press.

ESCAP/WMO Typhoon Committee (2000), New weather systems inaugurated, *Newsletter*, **12**: 6.

Fisher, E. L. and Caplan, P. (1963), An experiment in the numerical prediction of fog and stratus, *J. Atmos. Sci.*, **20**: 425—437.

Fletcher, N. H. (1966), *The Physics of Rainclouds*, Cambrige Universitatis Press, pp. 1—30.

Grell, G. A., Dudhia, J. et al. (1995), A Description of the Fifth-Generation Penn State/NCAR Mesoscale Model (MM5), NCAR/TN-398+STR (NCAR Technical Note), pp. 39—45.

Huang Jianping et al. (2000), A three-dimensional model study of complex terrain fog, *Chinese Journal of Atmospheric Sciences*, **24** (6): 821—834.

Jakob, C., Andersson, E. et al. (2000), The IFS cycle CY21r4 made operational in October 1999, *ECMWF Newsletter*, **87**: 2—9.

Mlawer, E. J., Taubman, S. J., Brown, P. D., Iacono, M. J. and Clough, S. A. (1997), Radiative transfer for inhomogeneous atmosphere: RRTM, a validated correlated-k model for the longwave, *J. Geophys. Res.*, **102** (D14): 16663—16682.

Qian Minwei et al. (1990), A numerical study of radiation fog over Changjiang River, *Chinese Journal of Atmospheric Sciences*, **14** (4): 483—489 (in Chinese).

Roach, W. T. and Brown, R. (1976), The physics of radiation fog: 2-D numerical study, *Quart. J. R. Meteor. Soc.*, **102**: 335—354.

Shi Chun'e, Li Zihua et al. (1996), 3D model study on fog over complex terrain, Part I: Numerical study, *Acta Meteor. Sin.*, **10** (4): 493—506.

Tang Haohua, Fan Shaojia et al. (2002), Research of the microphysical structure and evolution of dense fog over Nanling Mountain area, *Acta Scientiarum Naturalium Universitatis Sun Yat-Seni*, (4): 92—97 (in Chinese).

Tourskoi, P. (1967), *Meteorology*, Commercial Press, pp. 173—175.

White, B. G., Paegle, J. et al. (1999), Short-term forecast validation of six models, *Weather and Forecastong*, **14**: 84—108.

Zdunkowski, W. G. and Nielsen, B. C. (1969), A preliminary predication analysis of radiation fog, *Pure Appl. Geophys.*, **75**: 278—299.

Zhang Liming et al. (1993), A two-dimensional time-integral numerical model of Chongqing fog *Chinese Journal of Atmospheric Sciences*, **17** (6): 750—755 (in Chinese).

Zhou Binbin (1987), The simulation modeling of radiation fog, *Acta Meteor. Sinica*, **45**: 21 — 29 (in Chinese).